



RESEARCH ARTICLE

Model-based analysis of the influence of surface roughness on fatigue processes

Sikang Yan¹  | Arsalan Jawaid²  | Eberhard Kerscher³ | Jörg Seewig² | Ralf Müller¹

¹Institute for Mechanics, Technical University of Darmstadt, Darmstadt, Germany

²Institute for Measurement and Sensor Technology, RPTU Kaiserslautern-Landau, Kaiserslautern, Germany

³Working Group Materials Testing, RPTU Kaiserslautern-Landau, Kaiserslautern, Germany

Correspondence

Sikang Yan, Institute for Mechanics, Technical University of Darmstadt, Darmstadt, Germany.
Email: sikang.yan@tu-darmstadt.de

Funding information

Deutsche Forschungsgemeinschaft, Grant/Award Number: 252408385-IRTG 2057

Abstract

In the last decade, the phase field method was developed to simulate fatigue fracture processes. The biggest advantage of phase field modeling is its unified framework, in which the entire fracture evolution from nucleation to propagation is covered. Even though it is known that surface roughness has an essential impact on fatigue life, it has rarely been considered directly in phase field models for fatigue processes due to the required computational effort. In this work, we provide a simulation setup to incorporate roughness profiles into a phase field model for fatigue cracks. We have used a roughness model for our studies and also present initial results that show agreement between simulation and experiments.

1 | INTRODUCTION

Fatigue failure is one of the most crucial issues in manufacturing and engineering scenarios. Stress or displacement cycles can cause cracks to form and grow, eventually leading to the failure of the structure. However, predicting fatigue failure is extremely difficult because it usually does not happen immediately but rather after tens of thousands or millions of cycles of repeated loading. Originating from the energy criterion of Griffith [1], the phase field method [2, 3] points out a simple approach to simulate fatigue fracture. The phase field model directly incorporates the variational form of the total energy [4], and the crack status is indicated by a scalar variable. There are different phase field formulations for fatigue fracture simulation; peculiarly, Schreiber et al. proposed a phase field fatigue model by introducing an additional fatigue crack driving force [3]. Later, this phase field fatigue formulation has been successfully extended to include complex loading situations [5], adaptive simulation schemata [6], thermomechanical fatigue [7] and it is also able to be explained by the configurational force framework [8].

On the other hand, the significance of surface roughness extends across various scientific fields [9], with fatigue behavior being one particular application. Investigations showed a considerable impact of surface roughness on fatigue life [10, 11].

This is an open access article under the terms of the [Creative Commons Attribution-NonCommercial](https://creativecommons.org/licenses/by-nc/4.0/) License, which permits use, distribution and reproduction in any medium, provided the original work is properly cited and is not used for commercial purposes.

© 2024 The Author(s). *Proceedings in Applied Mathematics & Mechanics* published by Wiley-VCH GmbH.

Nevertheless, verifying the impact of surface roughness on fatigue behavior through experiments is challenging, as it necessitates the manufacturing of predefined surface roughness. Using simulation data instead of real data can bridge the comprehension gap between surface texture and the fatigue process more efficiently. A recent method that provides a comprehensive model for surface roughness employs a Gaussian process and a noise model [12]. This approach enables the simulation of specific structures, facilitating the analysis of their impact on fatigue behavior.

In this paper, we combine the two above-mentioned methods and present a computationally affordable setup that mimics a classic fatigue test experiment. An initial analysis of the effect of surface roughness on the fatigue life is also provided. The outline of the paper is as follows: In Sections 2 and 3, the phase field model for fatigue fracture and the roughness model for surface texture are both stated. In Section 4, we describe the experimental setup and use those approaches to analyze the fatigue life of the rough surface. In Section 5, the conclusion and the direction for future work are given.

2 | A PHASE FIELD MODEL FOR CYCLIC FATIGUE

The phase field model introduces an additional continuous crack field variable to represent the status of the damage to the material [2]. In the presented phase field model, we use a crack field s to indicate that: if this crack field s is 1, then the material is undamaged; and if it is 0, then cracks occur. The crack evolution is governed by the variational principle of the total energy \mathcal{E} of a loaded body Ω . Let \mathbf{t} be the external traction and \mathbf{f} the volume forces on the body, the total energy of the body is given as

$$\mathcal{E} = \int_{\Omega} \psi \, dV - \int_{\partial\Omega} \mathbf{t} \, dA - \int_{\Omega} \mathbf{f} \, dV. \quad (1)$$

Here, the variable ψ denotes the total energy density of the body, which consists of three parts [3]

$$\psi(\boldsymbol{\varepsilon}, s, \nabla s, D) = (g(s) + \eta)\psi^e(\boldsymbol{\varepsilon}) + \psi^s(s, \nabla s) + h(s)\psi^{\text{ad}}(D), \quad (2)$$

where the functions $g(s)$ and $h(s)$ are the degradation functions, modeling the loss of the stiffness of the broken material, and η is a numerical parameter for the stability of the model by providing a residual stiffness in the crack region.

The strain energy density

$$\psi^e(\boldsymbol{\varepsilon}) = \frac{1}{2} \boldsymbol{\varepsilon} : (\mathbb{C}\boldsymbol{\varepsilon}) \quad (3)$$

is taken from the hyper-elastic energy density functional, where $\boldsymbol{\varepsilon}$ is the infinitesimal strain [13].

The crack surface energy density

$$\psi^s(s, \nabla s) = G_c \left(\frac{(1-s)^2}{4\epsilon} + \epsilon |\nabla s|^2 \right) \quad (4)$$

models the energy required to separate the material and to generate cracks [14]. The parameter G_c is the critical energy release rate, which can be understood as the fracture resistance. The length parameter ϵ controls the width of the smooth transition zone between the broken and undamaged material.

The additional fatigue energy density

$$\psi^{\text{ad}}(D) = q \langle D - D_c \rangle^b \quad (5)$$

accounts for the accumulated fatigue driving force, which is related to a fatigue damage parameter D . This fatigue damage parameter will be accumulated during the entire simulation $D = D_0 + dD$, where the parameter D_0 is the previous damage and dD is the damage increment, which is given as $dD = \frac{dN}{n_D} \left(\frac{\hat{\sigma}}{A_D} \right)^k$. The damage increment dD contains the parameters n_D , A_D , and k of the SN-diagram from life time experiments [15], whereas dN denotes the cycle increment. The presented phase field simulation is followed by an adaptive cycle number adjustment algorithm (ACNAA) [6], in which the cycle increment dN is associated with the damage increment dD to ensure an optimized computing time. The parameter $\hat{\sigma}$ is

the fatigue driving force, and here the first principal stress is taken. The parameter D_c together with the Macaulay brackets $\langle \cdot \rangle$ defines a threshold, where this fatigue energy will not be considered unless the damage parameter D is bigger than this threshold. The other parameters b and q in Equation (5) are numerical parameters, controlling the speed of the energy growth. With the variational principle, minimizing the total energy by the crack field s and strain tensor ε yields four coupled governing equations to simulate the fatigue fracture [6]

$$\operatorname{div} \frac{\partial \psi}{\partial \nabla \mathbf{u}} = 0 \quad (6)$$

$$\frac{\partial \psi}{\partial s} - \operatorname{div} \frac{\partial \psi}{\partial \nabla s} = 0 \quad (7)$$

$$\frac{\partial \psi}{\partial \nabla s} \cdot \mathbf{n} = 0 \quad \text{on } \partial \Omega_{\nabla s} \quad (8)$$

$$\left(\frac{\partial \psi}{\partial \nabla \mathbf{u}} \right)^T \mathbf{n} = \mathbf{t} \quad \text{on } \partial \Omega_t, \quad (9)$$

With constitutive law [13], Equation (6) can be rewritten as

$$\operatorname{div} \boldsymbol{\sigma} = 0, \quad (10)$$

describing the equilibrium of the stress field $\boldsymbol{\sigma}$. The next equation (Equation 7) can be further extended to a regularized [16], providing the evolution equation of the crack field

$$\frac{ds}{dN} = -M \frac{\delta \psi}{\delta s} = -M \left(\frac{\partial \psi}{\partial s} - \operatorname{div} \frac{\partial \psi}{\partial \nabla s} \right), \quad (11)$$

where $M > 0$ is a mobility parameter, which models the “viscosity” (rate dependency) of the phase field fracture model. The last two equations (Equations 8 and 9) define the boundary conditions for the crack field and the stress field on boundaries $\partial \Omega_{\nabla s}$ and $\partial \Omega_t$, where \mathbf{n} denotes the outward normal vector to the domain.

3 | ROUGHNESS MODEL

Typically modeled as a stochastic process, surface roughness is described by its amplitude distribution and spatial correlations [17]. Jawaid and Seewig used a Gaussian process and subsequent noise model approach to model surface texture [12]. The real-valued Gaussian process models the surface texture

$$G(x) \sim \mathcal{GP}(m(x), r(x, x')), \quad (12)$$

where $m(x) = \mathbb{E}[G(x)]$ is the expectation function and $r(x, x') = \mathbb{E}[(G(x) - m(x))(G(x') - m(x')))]$ is the autocovariance function. Whereas, the noise model can be interpreted to resemble measurement noise or generally any stochasticity of the surface texture of the workpiece

$$\mathbf{Z} \sim p(\mathbf{z}|\mathbf{g}), \quad (13)$$

where $\mathbf{Z} \in \mathbb{R}^{n_p}$ is the surface texture, $\mathbf{g} \in \mathbb{R}^{n_p}$ is a sampled Gaussian process from Equation (12), and n_p denotes the number of sampling points on the surface. The simulation of the Gaussian process is performed by a realization of a multidimensional Gaussian distribution. We refer to the refs. [12, 18] for a more concise discussion on the modeling and simulation approach of surfaces with Gaussian processes.

For the purposes of this work, we looked at engineering parts that are manufactured by turning processes. Furthermore, we considered only profile traces of the surfaces in our studies, and we denote them as turned profiles. To simulate these profiles, we need to take their features into account. Turned profiles have periodic features that alternate between narrow hills and wide dales. Thus, we modeled them with Gaussian processes with the following periodic autocovariance

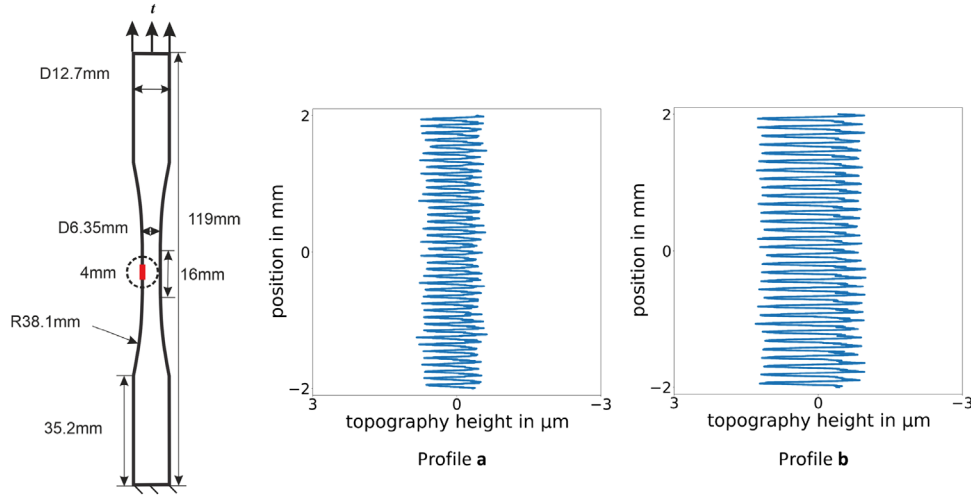


FIGURE 1 The fatigue test specimen, in which the marked area (in red) is set up with different types of roughness. The roughness profiles are simulated by using the parameters listed in Table 1.

function [19]

$$r(x, x') = \sigma^2 \exp \left(-\frac{1}{2} \left(\frac{\sin \left(\frac{\pi}{\lambda} (x - x') \right)}{\theta} \right)^2 \right), \quad (14)$$

with σ^2 the variance, θ the length-scale, λ the period. We used an additive Gaussian process as a noise model that includes colored noise with small correlation lengths in the simulations. For example, colored noise describes small surface defects caused by tool vibrations during manufacturing, resulting in more realistic turned profiles. The noise model has the standard squared-exponential autocovariance function

$$r_{\text{noise}}(x, x') = \sigma_n^2 \exp \left(-\frac{1}{2} \left(\frac{(x - x')}{\theta_n} \right)^2 \right), \quad (15)$$

where σ_n^2 is the noise variance and θ_n is the noise length-scale with $\theta_n \ll \theta$. The expectation functions of both Gaussian processes are constant functions with $m(x) = m_{\text{noise}}(x) = 0$. These parameters allow the simulation of profiles with targeted features. For example, the variance σ^2 and the period λ are strongly correlated with feature heights and spacings, respectively. Regarding simulations, all Gaussian process simulations are performed by applying the contour integral quadrature method [20] with 100 Krylov iterations and 8 quadrature points.

4 | ON THE PHASE FIELD SIMULATION OF ROUGH SURFACE PROFILES

In this section, classic fatigue test experiments ASTM-E606 are carried out by the presented phase field model. The dimension of the specimen is reported in Figure 1. The roughness of the surface of the specimen is considered in the phase field simulation, which is modeled by a Gaussian process and a noise model introduced in Section 3. The rough surface is assumed to only appear in the red area in the middle of the left side of the specimen (4 mm) as shown in Figure 1. We simulated two turned profiles by the roughness model with two different sets of parameters in this work, as shown in Table 1. Compared to profile **a**, profile **b** has higher roughness values R_a and R_z . For the sake of limiting the computational effort, only the area with roughness influence is explicitly simulated using the phase field model as shown in Figure 2. This approximation yields simulations with the same qualitative result as using the specimen geometry of ASTM-E606. This is due to the fact that the crack will usually nucleate in the thinned area of the specimen. To solve the phase field governing equations properly and fully capture the roughness details, the elements of the left end of the square have been refined to

TABLE 1 Parameters of simulated turned profiles with the model according to Section 3.

Parameters	Profile a	Profile b
Variance $\sigma^2/\mu\text{m}^2$	1	2
Length-scale θ	$\sqrt{5/4}$	$\sqrt{5/8}$
Period λ/mm	1/10	1/8
Variance of noise model $\sigma_n^2/\mu\text{m}^2$	1/10	1/10
Length-scale of noise model θ_n/mm	1/400	1/400

Note: A simulated profile has $n_p = 8000$ sampling points with a sampling distance $x_{i+1} - x_i = 5 \times 10^{-4}$ mm for $i = 0, \dots, n_p - 2$.

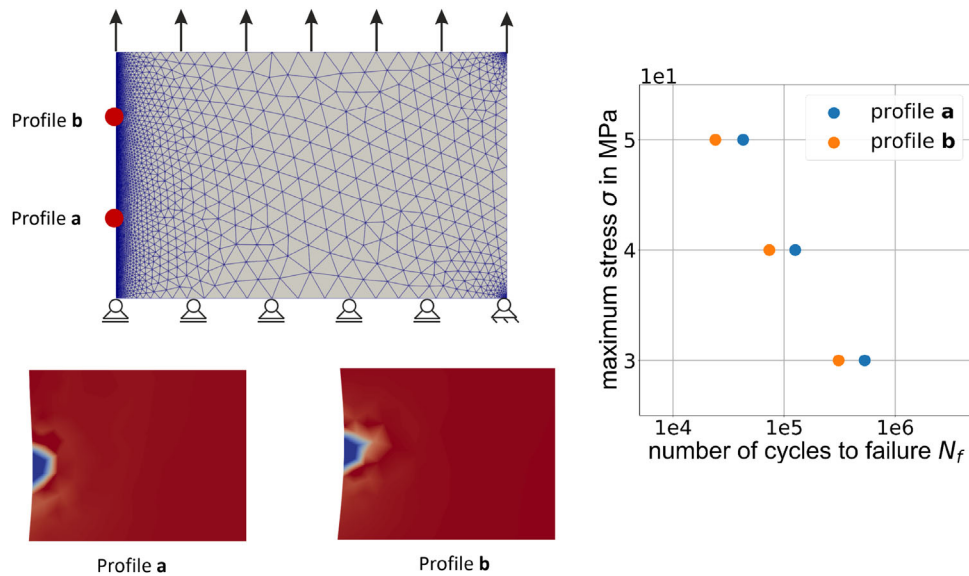


FIGURE 2 On the left is one mesh for the phase field simulation. The fatigue cracks from these profiles nucleate at different locations on the surface, indicated by red dots in the mesh. The crack nucleates at -0.5020 mm in profile **a** and at -0.5245 mm in profile **b**. The cracks for both profiles are visualized at the bottom ($s = 1$ is red, $s = 0$ is blue). On the right, the fatigue life for both profiles is shown in an SN diagram.

a size of 5×10^{-4} mm. Since the boundary conditions are inherited from the original fatigue test problem, the top of the square is given a tension load, and the bottom of the square is constrained in the vertical direction with the horizontal direction free. To avoid rigid body motion, the right bottom corner is additionally fixed in both directions. It is important to note that the fatigue cracks are nucleated at different positions of the surfaces in the simulation for the two profiles. The positions are indicated by red dots in the mesh of Figure 2. This difference is explained by the fatigue driving force of the model [6], where the crack nucleation is triggered by the (maximum) first principal stress. Furthermore, the right side of Figure 2 shows the fatigue life of these specimens assembled in an SN diagram with both roughness profiles.

In the following, we qualitatively reproduce the results with our simulations from previously published physical experiments [21, 22], which showed that fatigue life decreases with increasing height-specific roughness parameters (e.g., R_a , R_t , R_z). Thus, we scale the topography heights of both surface profiles with three different magnitudes (0.5, 1.0, 2.0) as shown in Figure 3. The simulation results are depicted in Figure 4. Our results confirm that increasing the topography heights or height-specific parameters will decrease the fatigue life of the specimen. This can be explained again by the performance of the fatigue driving force, where a higher driving force is generated by increasing the topography height, which leads to a shorter fatigue life. In Table 2 detailed information regarding fatigue life and relative fatigue driving force using profile **a** is provided. In the meantime, although the fatigue lives are different within the scaled surface profile, the location of the first nucleated crack can be found at the same position as depicted in Figure 5. Consequently, our experiments indicate that the fatigue driving force is also dependent on the spatial attributes of surface features.

We confirmed by these simulations that as the value of the roughness parameter R_z or R_a increases, the specimen will experience a shorter fatigue life. However, these parameters do not characterize the spatial features of the surface, which clearly indicate the position of the crack nucleation. Considering both surface properties (height and spatial) will provide

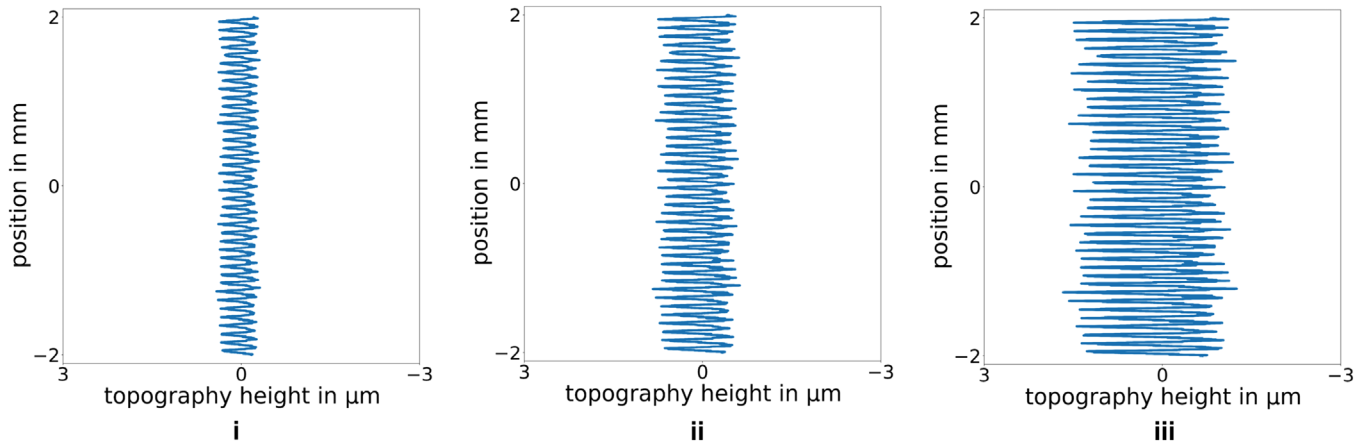


FIGURE 3 An example of scaling using profile **a**. The simulated surface texture is scaled with different factors to amplify the influence from topography heights (**i**: scaling with 0.5; **ii**: original surface profile; **iii**: scaling with 2).

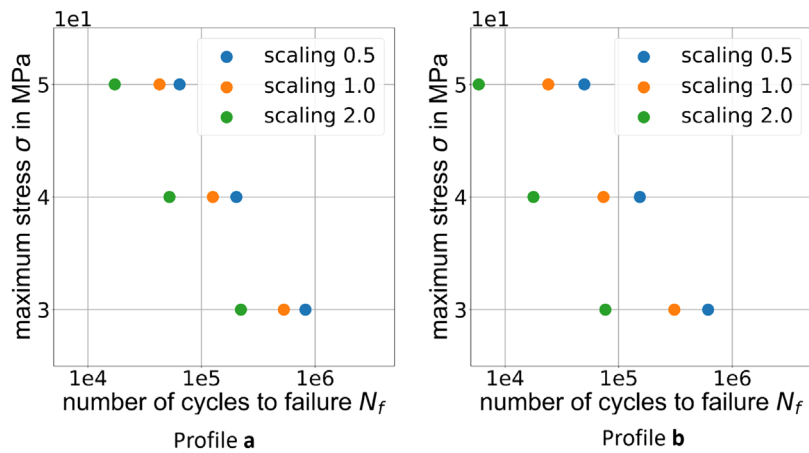


FIGURE 4 Fatigue lives with different scaling of the two profiles **a** and **b** in SN diagrams.

TABLE 2 The relation between fatigue life and fatigue driving force by different topography heights using the example of profile **a**.

Scaling factor	Fatigue life	Relative driving force in %
0.5	180453	93.3
1.0	125764	100.0
2.0	32467	132.6



FIGURE 5 The first crack can be found at the same position (**i**: scaling with 0.5; **ii**: original surface profile; **iii**: scaling with 2) using an example of profile **a**. Red indicates a crack field variable of $s = 1$ and blue indicates $s = 0$.

more insights into fatigue life. In all, it is shown that a surface with sharp dales leads to a higher stress concentration in the profiles due to the notch effect, which finally triggers the specimen to initiate a crack, let it grow, and finally fracture. Similar experimental observations can be found in ref. [10].

5 | CONCLUSION

The phase field model for fatigue fracture has been widely deployed for scientific computing due to its simple and elegant form. However, despite the well-established phase field model, there is still a lack of studies on how surface roughness influences fatigue life. In this work, we incorporated a roughness model, which uses a Gaussian process and a noise model to enclose the surface roughness effect in phase field computing. Results show that surfaces with higher roughness reduce the fatigue life of specimens, which is in agreement with experimental observation.

ACKNOWLEDGMENTS

This work is funded by the Deutsche Forschungsgemeinschaft (DFG, German Research Foundation)–252408385–IRTG 2057.

ORCID

Sikang Yan  <https://orcid.org/0000-0003-3615-889X>

Arsalan Jawaid  <https://orcid.org/0000-0001-9951-4164>

REFERENCES

1. Griffith, A. A. (1921). Vi. the phenomena of rupture and flow in solids. *Philosophical transactions of the royal society of london. Series A, containing papers of a mathematical or physical character*, 221(582-593), 163–198.
2. Kuhn, C., & Müller, R. (2010). A continuum phase field model for fracture. *Engineering Fracture Mechanics*, 77(18), 3625–3634.
3. Schreiber, C., Kuhn, C., Müller, R., & Zohdi, T. (2020). A phase field modeling approach of cyclic fatigue crack growth. *International Journal of Fracture*, 225(1), 89–100.
4. Bourdin, B., Francfort, G. A., & Marigo, J. J. (2000). Numerical experiments in revisited brittle fracture. *Journal of the Mechanics and Physics of Solids*, 48(4), 797–826.
5. Schreiber, C., Müller, R., & Kuhn, C. (2021). Phase field simulation of fatigue crack propagation under complex load situations. *Archive of Applied Mechanics*, 91, 563–577.
6. Yan, S., Schreiber, C., & Müller, R. (2022). An efficient implementation of a phase field model for fatigue crack growth. *International Journal of Fracture*, 237, 47–60.
7. Yan, S., Müller, R., & Ravani, B. (2024). Thermomechanical fatigue life simulation using the phase field method. *Computational Materials Science*, 235, 112829.
8. Yan, S., Schlüter, A., Faust, E., & Müller, R. (2023). Configurational forces in a phase field model for the cyclic fatigue of heterogeneous materials. *Forces in Mechanics*, 13, 100239.
9. Pawlus, P., Reizer, R., & Wiczorowski, M. (2021). Functional importance of surface texture parameters. *Materials*, 14(18), 5326.
10. Taylor, D., & Clancy, O. (1991). The fatigue performance of machined surfaces. *Fatigue & Fracture of Engineering Materials & Structures*, 14(2-3), 329–336.
11. Li, C., Dai, W., Duan, F., Zhang, Y., & He, D. (2017). Fatigue life estimation of medium-carbon steel with different surface roughness. *Applied Sciences*, 7(4), 338.
12. Jawaid, A., & Seewig, J. (2023). Model of rough surfaces with Gaussian processes. *Surface Topography: Metrology and Properties*, 11(1), 015013.
13. Spencer, A. J. M. (2004). *Continuum mechanics*. Courier Corporation.
14. Bourdin, B., Francfort, G. A., & Marigo, J. J. (2008). The variational approach to fracture. *Journal of Elasticity*, 91(1-3), 5–148.
15. ASTM E606/E606M-12 . (2021). *Standard test method for strain-controlled fatigue testing*. ASTM International, West Conshohocken, PA. https://doi.org/10.1520/E0606_E0606M-21
16. Gurtin, M. E. (1996). Generalized Ginzburg-Landau and Cahn-Hilliard equations based on a microforce balance. *Physica D: Nonlinear Phenomena*, 92(3-4), 178–192.
17. Whitehouse, D. J., & Archard, J. F. (1970). The properties of random surfaces of significance in their contact. *Proceedings of the Royal Society of London A: Mathematical and Physical Sciences*, 316(1524), 97–121.
18. Jawaid, A., & Seewig, J. (2023). Discrete filter and non-gaussian noise for fast roughness simulations with gaussian processes. *Proceedings of the 3rd Conference on Physical Modeling for Virtual Manufacturing Systems and Processes*. Springer International Publishing.
19. MacKay, D. J. C. (1998). Introduction to Gaussian processes. In C. M. Bishop (Ed.) *Neural Networks and Machine Learning* (pp. 133–166). NATO ASI Series.

20. Pleiss, G., Jankowiak, M., Eriksson, D., Damle, A., & Gardner, J. R. (2020). Fast matrix square roots with applications to gaussian processes and bayesian optimization. *Advances in neural information processing systems*. Curran Associates, Inc.
21. Li, C., Dai, W., Duan, F., Zhang, Y., & He, D. (2017). Fatigue life estimation of medium-carbon steel with different surface roughness. *Applied Sciences*, 7(4), 338.
22. Yadollahi, A., Mahtabi, M., Khalili, A., Doude, H., & Newman Jr, J. (2018). Fatigue life prediction of additively manufactured material: Effects of surface roughness, defect size, and shape. *Fatigue & Fracture of Engineering Materials & Structures*, 41(7), 1602–1614.

How to cite this article: Yan, S., Jawaid, A., Kerscher, E., Seewig, J., & Müller, R. (2024). Model-based analysis of the influence of surface roughness on fatigue processes. *Proceedings in Applied Mathematics and Mechanics*, 24, e202400039. <https://doi.org/10.1002/pamm.202400039>